Journal of Traditional and Complementary Medicine 11 (2021) 446–456

Contents lists available at ScienceDirect

Journal of Traditional and Complementary Medicine

journal homepage: http://www.elsevier.com/locate/jtcme

Original Article

Wound healing activity of the hydroethanolic extract of the leaves of *Maytenus ilicifolia* Mart. Ex Reis

Francyelle Borges Rosa de Moura [a, b], Bruno Antonio Ferreira [a, c], Simone Ramos Deconte [a], Breno Costa Landim [a], Allisson Benatti Justino [c], Andrea Aparecida de Aro [b], Foued Salmen Espindola [c], Rodney Alexandre Ferreira Rodrigues [d], Daniele Lisboa Ribeiro [a], Fernanda de Assis Araújo [a], Tatiana Carla Tomiosso [a, *]

[a] *Institute of Biomedical Sciences, Federal University of Uberlândia, Avenue Pará 1720, zip code 38400-902, Uberlândia, MG, Brazil*
[b] *Institute of Biology, State University of Campinas, Street Monteiro Lobato, 255, zip code 13083-862, Campinas, SP, Brazil*
[c] *Institute of Biotechnology, Federal University of Uberlândia, Street Acre 1004, zip code 38405-319, Uberlândia, MG, Brazil*
[d] *Multidisciplinary Center of Chemical, Biological and Agricultural Research, State University of Campinas, Street Alexandre Cazelatto 999, zip code 13148-218, Paulínia, SP, Brazil*

ARTICLE INFO

Article history:
Received 16 October 2020
Received in revised form
15 March 2021
Accepted 26 March 2021
Available online 30 March 2021

Keywords:
Celastraceae
Collagen
Inflammation
Medicinal plants
Polyphenol

ABSTRACT

Background and Aim: Maytenus ilicifolia has analgesic, healing, antioxidant and anti-inflammatory properties. This study evaluated effect of the hydroalcoholic extract of *M. ilicifolia* leaves on skin wound repair.

Experimental procedure: Wounds were induced on mice and treated with the extract. The treatment was performed daily, until day 7 after wound induction. Wound closure was measured and the features of the repaired tissue were investigated, including mast cell quantification, neutrophil and macrophage activities, collagen deposition, angiogenesis, and pro-metalloproteases and metalloproteases 2 and 9 activity (pro-MMPs and MMPs).

Results and conclusion: The *M. ilicifolia* extract accelerated the closure of wounds. The extract at a concentration of 4% was found to be effective, presenting anti-inflammatory effects and hemoglobin increased, along with increased soluble, total and type III collagens in the wound. In addition, there was an increase in pro-MMP9 and MMP9 activity after day 7th of treatment. The phenolic compounds and tannins present in this plant could be associated with the anti-inflammatory and healing activities observed in this study. Therefore, the ability to modulate essential parameters for accelerated and adequate healing as shown here suggests that the use of standardised extracts of *M. ilicifolia* and its fractions enriched in polyphenols may represent a therapeutic strategy for the treatment of wounds.

1. Introduction

When damaged, the skin restores its morphology and function through the healing process, a physiological event.[1] However chronic conditions, such as diabetes mellitus, peripheral vascular disease and pressure ulcers, can compromise the quality and resolution of wound healing.[2] Wounds that do not heal generate considerable economic expense. For example, total expenditures in the United States for all types of wounds are estimated to range from $28.1 to $96.8 billion.[3] Patients with persistent wounds represent about 1%–2% of the general population in developed countries.[4,5]

Abbreviations: **Hb**, Hemoglobin; **MiHE**, Maytenus ilicifolia hydroethanolic extract; **MMP2**, metalloprotease 2 active; **MMP9**, metalloprotease 9 active; **MPO**, myeloperoxidase; **NAG**, *N*-acetyl-beta-D-glucosaminidase; **Pro-MMP2**, pro-metalloprotease 2; **Pro-MMP9**, pro-metalloprotesase 9.

* Corresponding author. Instituto de Ciências Biomédicas, Departamento de Histologia, Universidade Federal de Uberlândia, Avenida Pará 1720 – Bloco 2B, CEP 38400-902, Uberlândia, Brazil.
E-mail address: tatianatomiosso@ufu.br (T.C. Tomiosso).

Peer review under responsibility of The Center for Food and Biomolecules, National Taiwan University.

https://doi.org/10.1016/j.jtcme.2021.03.003

Considering the available forms of treatment, only 1–3% of modern medicines are used for the treatment of wounds and skin diseases, while about one third of all herbal medicines are used for these treatments.[6] For this reason, a survey of plant extracts remains a viable strategy in the search for new and efficient therapeutic agents for wound repair, as with the use of *Zataria multiflora*, *Teucrium polium*, *Aloe vera* and *Annona crassiflora*.[7–10] *Maytenus ilicifolia* Mart. ex Reissek, popularly known as espinheira santa, is a plant described in traditional medicine with scientific evidence for antiulcerogenic, anti-inflammatory and healing properties.[11,12] In addition, the use of this plant has a scientifically proven analgesic effect.[12]

In the present study, we identified polyphenols, flavonoids and tannins in *M. ilicifolia* hydroalcoholic extract (MiHE), in addition to organic acids (malic and citric acid). The anti-inflammatory,[13] antioxidant[14] and astringent properties[15] are described for these compounds and may contribute to the repair of wounds. Commercialisation of *M. ilicifolia* as an herbal medicine is standardised according to the content of tannins, and approved by the Agência Nacional de Vigilância Sanitária Brazilian (ANVISA). **S**tudies have evaluated and reinforced the safety in the use of this plant in different experimental models.[16–20] Tannins have healing properties, as they promote the precipitation of proteins leading to the appearance of a protective layer that can improve the regenerative process.[21] Despite this, to date, studies on the pharmaceutical potential of the bioactive compounds of *M. ilicifolia* have only addressed the forms used in the healing of gastric ulcers. Studies of its effect on the healing of skin wounds have not yet been published.

Thus, the present investigation is the first study to evaluate the effects of the hydroalcoholic extract of *M. ilicifolia* leaves on skin wound repair. For this purpose, the ability of *M. ilicifolia* extract to modulate the inflammatory response, angiogenesis, collagen deposition, matrix metalloproteases activities (MMP-2 and MMP-9) and time required for wound closure were considered.

2. Materials and methods

2.1. Preparation of hydroethanolic extract of M. ilicifolia leaves

M. ilicifolia leaves were collected in the Multidisciplinary Center of Chemical, Biological and Agricultural Research of the State University of Campinas in Paulinia, Brazil. A voucher specimen was identified and deposited in the Herbarium of the University State of Campinas (register 112745). The hydroethanolic extract of *M. ilicifolia* leaves was used for the treatment of wounds, named here as MiHE. The extraction of the compounds was obtained after six days of maceration with 600 g of leaves of *M. ilicifolia* in 4 L of 70% ethanol in distilled water (70:30). After this period, the solution was filtered and the alcohol evaporated in a rotary evaporator (R-200 Advanced) at 40 °C. The extract obtained (MiHE) was frozen and lyophilized (L101 Liobras ®) to remove residual water .[22,23]

2.2. Liquid chromatography-mass spectrometry analysis

The main compounds of MiHE were identified by high-performance liquid chromatography coupled to a mass spectrometer with electrospray ionization (HPLC-ESI-MS/MS, Agilent Q-TOF, model 6520). MeOH–H_2O (4:1) was used as solvent system and the sample was infused into the ESI source at a flow rate of 200 μL/h. Nitrogen gas was used as drying gas at a flow rate of 8 L/min and as nebulizer gas at 58 psi. The temperature of nebulizer was set at 200 °C and a potential of 4.5 kV was applied in the capillary. The electron impact energy was set at 5–30 eV. The HPLC parameters were: Agilent Zorbax model 50 × 2.1 mm column, particles of 1.8 μm and pore diameter of 110 Å, mobile phase: water acidified with formic acid (0.1% v/v) (A) and methanol (B). The gradient solvent system (B) was: 2% (0 min); 98% (0–15 min); 100% (15–17 min); 2% (17–18 min); 2% (18–22 min), with a flow of 0.35 mL/min and detection at UV of 280 and 360 nm. The data were acquired in negative and positive modes, with adjustment for a range of 20–1000 *m/z*.

2.3. Wound induction

For wound creation, the animals were anesthetized with ketamine (100 mg/kg) and xylazine (10 mg/kg) intraperitoneally. Ketamine and xylazine were obtained from Syntec®.The dorsal region of each animal was trichotomized and four wounds were produced in this region with a 5 mm punch. The wounds were made equidistant with about 1 cm of distance between them. All animals were housed in individual cages after surgery avoiding any external intervention that could compromise the results.

2.4. Groups and treatments

All animal procedures were approved by the Ethics Commission of Animal Use of the Federal University of Uberlandia with the registration of protocol number 062/16 (june17, 2016). Sixty-four male BALB/c mice, healthy, weighing approximately 27 g at nine weeks of age, were used in the experiments. The animals were created, provided and kept in the Rede de Biotérios de Roedores of the Federal University of Uberlandia (REBIR-UFU) under standard conditions (22 ± 1 °C, humidity 60 ± 5% and 12 h of light/12 h of darkness), and fed standard laboratory chow and tap water ad libitum. The animals were randomly divided as described in Table 1.

For treatment, MiHE was pulverized in a pestle and mortar and subsequently incorporated into vaseline and lanolin at concentrations of 2%, 4%, and 6%. The animals of the control group had their wounds treated with vehicle (vaseline and lanolin).[10,24,25] Thirty minutes after wound creation, 100 mg of the ointment was topically applied on each wound. The wound induction, treatment and euthanasia were performed in the morning. The treatments were performed once a day, for 3 or 7 days. The treatment was completed without loss of animals.

2.5. Wound closure

Wound size was measured using a digital caliper (150 mm-Matrix) after the induction of the wound and at the 3rd and 7th days post-surgery, before the ointment application, in order to compute the wound area. Further, digital photographs of the wounds were taken (Sony Cyber Shot 14.1 Dsc W320). The percentage of wound closure was calculated using the following formulas[26]:

*Wound area: (smaller diameter/2) * (larger diameter/2) *π*

Area measurement (%): % wound closure = [1-(Wa)/(Wa0) X 100], where Wa: wound area and Wa0: original area of the wound area.

2.6. Tissue collection

Animals were euthanized at the pre-determined time points, three and seven days after wound creation with thiopental (Thiopental®) via intraperitoneal route (100 mg/kg). The wounds were removed using a 5 mm punch and immediately put into methacarn (methanol, acetic acid, and chloroform in the proportion of 6:3:1, respectively) for 3 h, and then directed to the histological process.

Table 1
Description and distribution of the evaluated groups (treated groups and control group).

Groups	Description	Number of animals for treatment time	
		3 days	7 days
CO	Animals injured and treated with the vehicle (vaseline 70%/lanolin 30%).	8	8
2% MiHE	Animals injured and treated with *M. ilicifolia* extract hydroalcoholic at 2% concentration.	8	8
4% MiHE	Animals injured and treated with *M. ilicifolia* extract hydroalcoholic at 4% concentration.	8	8
6% MiHE	Animals injured and treated with *M. ilicifolia* extract hydroalcoholic at 6% concentration.	8	8
		Total	**64 animals**

Otherwise, samples for biochemical evaluation were preserved in an ultra-freezer at −80 °C until analysis.

2.7. Myeloperoxidase activity (MPO)

Neutrophil infiltration in wounds were indirectly measured by assaying MPO activity as a quantitative marker of the activity of this cell type.[27] One wound of each animal was weighed and homogenized in 2 mL of 80 mM sodium phosphate buffer at a pH of 6 for 15 s. Then, 300 μl of the sample were transferred to an microtube with 600 μL of HTAB (Hexade-Cyltrimethylammonium Bromide; Sigma-Aldrich) 0.75% w/v diluted in phosphate buffer at pH 6. Samples were sonicated for 10 s and centrifuged at 2.700×*g*, for 10 min at 4 °C. The supernatant (200 μL) was used in the enzymatic assays. The reaction followed the following order: 100 μL of 0.003% hydrogen peroxide; 100 μL of 6.4 mM TMB (3.3″,5.5″−tetramethylbenzidine; Sigma-Aldrich) diluted in DMSO (dimethyl sulfoxide; Merck), placed at the same time for 1 min timed. To stop the reaction, 100 μL of 4 M H_2SO_4 (sulfuric acid; Merck) were added in the mixture. Next, 200 μL of the samples were added in duplicates to a 96-well plate and the spectrophotometric reading was performed at 450 nm wavelength (E max, Molecular Devices). The results were expressed as MPO (absorbance in optical density/g wet weight of the sample).

2.8. N-acetyl-β-D-glycosaminidase activity (NAG)

The infiltrate of macrophage cells in wounds was quantified by measuring the levels of the lysosomal enzyme *N*-acetyl-β-D-glucosaminidase (NAG), which is present in high levels on activated macrophages.[28] This technique is based on the hydrolysis of *p*-nitrophenyl-*N*-acetyl-β-D-glucosamine (substrate) by *N*-acetyl-β-D-glucosaminidase and the release of *p*-nitrophenol. ½ wound of each animal was homogenized in 2.0 mL of 0.9% saline solution with 0.1% Triton X-100 (Promega), and then centrifuged at 960×*g* for 10 min at 4 °C. Next, 150 μL of the supernatant were added in 150 μL of citrate/phosphate buffer, and then, 100 μL of the mixture were added to a 96-well plate. Next, 100 μL of the substrate (*p*-nitrophenyl-*n*-acetyl-β-D-glucosaminidase; Sigma-Aldrich), diluted in citrate/phosphate buffer, pH 4.5, were incubated at 37 °C for 30 min. Then, 100 μL of 0.2 M glycine buffer (pH 10.6) were added into the samples. The absorbance was measured at 400 nm (E max, Molecular Devices). The analysis was performed in duplicate. The NAG activity was calculated from a standard curve of *p*-nitrophenol. The results were expressed as NAG (nmol/mg wet weight of the sample).

2.9. Mast cell quantification

For morphological analysis, ½ wound of each animal was fixed in methacarn and then embedded in paraffin. Longitudinal sections of 5 μm thickness were obtained in a rotary microtome (HM-315, MICROM). Histological sections were stained with 0.25% Toluidine Blue in a MacIlvaine pH 4.0 to determine the number of mast cells.[29] Ten areas of the wound were analyzed per animal. Photomicrographs were obtained with 400X magnification (40X objective) in Leica Microscope ICC50 (Leica Microsystems). All photomicrographs were quantified using Image J software for Windows (Image J bundled with 64-bit Java 1.8.0_112). The quantification of mast cells was performed with multipoint.

2.10. Metalloproteases activity (pro-MMPs and MMPs active 2 and 9)

MMPs activities were evaluated by gelatinolytic activity on zymography gel.[30,31] One wound was homogenized in extraction buffer for MMPs for 24 h (cacodylic acid, NaCl, CaCl2, NaN3, Triton 100X, ZnCl2). The sample were centrifuged at 10,000×*g* for 10 min and the supernatant was collected. Total protein in the samples was previously quantified[32] and 40 μg of proteins were separated by 10% SDS-PAGE (Sodium Dodecyl Sulfate/Polyacrylamide Gel Electrophoresis) containing 0.4% gelatin, at 4 °C and under nonreducing conditions. After electrophoresis, the gel was washed with 25% Triton X 100 buffer and incubated overnight at 37 °C with the incubation buffer (pH 7.4; 50 mM Tris−HCl, 10 nM $ZnCl_2$, 0.1 M NaCl and protease inhibitor). The gel was stained with 0.5% Coomassie Blue for 2 h and unstained with bleach solution (methanol/water/acetic acid in the ratio of 6: 3: 1, respectively). For this evaluation, a total of three animals per group were used and each gel was evaluated in duplicate. Gels were scanned and the activity of pro-MMPs and MMPs were evaluated by band densitometry in Image J software.

2.11. Hemoglobin measurement (Hb)

½ wound of each animal was individually homogenized (Ultra-turrax) into 2.0 mL of a hemoglobin-specific chromogenic reagent (Drabkin reagent-Labtest Hemoglobin Dosing Kit).[33,34] Next, the homogenized samples were centrifuged for 40 min at 10,000×*g* at 4 °C. The supernatants were filtered through 0.22 μm filters (Millipore) and 200 μL aliquot of each sample were added in duplicate to a 96-well plate. Hb concentration was determined spectrophotometrically by measuring absorbance at 540 nm (E max, Molecular devices). To calculate Hb concentration of each sample, a known standard curve (Labtest) was used. The content of Hb in each wound was expressed as μg Hb/mg of wet tissue.

2.12. Quantification of total collagen and type I and type III collagen

The sections of wounds used for the quantification of collagen were obtained according to the protocol previously mentioned for mast cells. Similarly, 10 areas of each photomicrograph were analyzed, one photomicrograph being analyzed for each animal. The slides obtained were stained with Sirius Red for quantification of total collagen and type I and III collagen.[29,35,36] For total collagen quantification, photomicrographs were obtained with 200X magnification (20X objective) in Nikon TS 100 microscope with

Optcam microcamera system. For collagen I and III quantification, a polarization filter was used. Before quantification, the image J program was calibrated with a gray scale. After converting the photomicrographs of total collagen into 8-bits, the tool threshold was used. For the quantification of collagen types I and III, these were initially differentiated with the Split Channels tool and then quantified by marking the area containing collagen with the Threshold tool. The relationship between the types of collagen was made by dividing the values of optical density of type I collagen by the values of type III collagen.

2.13. Soluble collagen measurement

Soluble collagen was measured by the reaction of Sirius Red.[37,38] ½ wound of each animal was homogenized into 1 mL of 0.1% Triton X-100 saline solution and then centrifuged at 6000×*g* for 10 min at 4 °C. Next, 50 μl of each sample were incubated with Sirius Red reagent for 30 min at room temperature (25 °C). Collagen-Sirius red complex was separated by centrifugation at 10,000×*g* for 10 min at 4 °C. The supernatant was discarded. The pellet was washed with 500 μL of ethanol (pure and methanol-free); after removing ethanol, the pellets were resuspended in 1 mL of alkaline solution (0.5 M NaOH). The absorbance was measured at 540 nm in a microplate reader (E max, Molecular Devices). The analysis was performed in duplicate. The amount of collagen in each sample was determined by comparing the results with a standard curve using collagen (Merk). The results were expressed in μg of collagen per mg of tissue sample.

2.14. Statistical analysis

All numerical data were tested for normal distribution using the Kolmogorov-Smirnov test. The results are presented as mean and ± error standard deviation (SEM), followed by One-Way ANOVA and Bonferroni post-tests, comparing treated groups (2% MiHE, 4% MiHE and 6% MiHE) with control group (CO group). Differences between standard error were considered significant when p values were ≤0.05. The statistical evaluation and graphs were performed using the GraphPad Prism software, version 8.0.

3. Results

3.1. Identification of polyphenols in MiHE

The compounds identified in MiHE by HPLC-ESI-MS/MS are shown in Table 2. The characterization demonstrated the presence

Table 2
Compounds identified in MiHE by HPLC-ESI-MS/MS (negative mode).

Compound identified	Retention time (min)	Formula $[M-H]^-$	Mass calculated for $[M-H]^-$	*m/z* of $[M-H]^-$	Error (ppm)	*m/z* of fragments of $[M-H]^-$	References
Malic acid	0.707	$C_4H_5O_5^-$	133.0142	133.0144	1.50	115, 114	https://www.sciencedirect.com/science/article/pii/S0308814607000702
Citric acid	0.841	$C_6H_7O_7^-$	191.0197	191.0200	1.57	165, 133, 111	https://www.ncbi.nlm.nih.gov/pubmed/27842248
(Epi)gallocatechin	4.003	$C_{15}H_{13}O_7^-$	305.0667	305.0666	−0.32	287, 219, 203, 167, 147, 125, 109	https://www.ncbi.nlm.nih.gov/pubmed/17851421
Type B proanthocyadinin (dimer)	4.202	$C_{30}H_{25}O_{11}^-$	561.1389	561.1397	1.42	517, 435, 289, 271, 203, 125	https://www.ncbi.nlm.nih.gov/pubmed/25032782
Type B procyanidin (dimer)	4.419	$C_{30}H_{25}O_{12}^-$	577.1351	577.1352	0.17	451, 407, 289, 245, 205, 161, 125	https://www.ncbi.nlm.nih.gov/pubmed/29425747
Type B proanthocyanidin (trimer)	4.735	$C_{45}H_{37}O_{16}^-$	833.2070	833.2078	0.96	707, 543, 407, 289, 125	https://www.ncbi.nlm.nih.gov/pubmed/25032782
(Epi)catechin	5.118	$C_{15}H_{13}O_6^-$	289.0718	289.0720	0.69	245, 203, 151, 109	https://www.ncbi.nlm.nih.gov/pubmed/27842248
Type B proanthocyanidin (trimer)	5.434	$C_{45}H_{37}O_{17}^-$	849.2026	849.2042	1.88	723, 559, 407, 289, 203, 125	https://www.ncbi.nlm.nih.gov/pubmed/25032782
Epiafzelechin	5.717	$C_{15}H_{13}O_5^-$	273.0761	273.0772	4.02	255, 227, 205, 187, 167, 109	https://www.ncbi.nlm.nih.gov/pubmed/25032782
Quercetin-rutinoside-glucoside	5.966	$C_{33}H_{39}O_{21}^-$	771.1989	771.1990	0.12	573, 505, 303, 301, 300, 255	https://www.ncbi.nlm.nih.gov/pubmed/18686968
Quercetin rhamnosylrutinoside	6.166	$C_{33}H_{39}O_{20}^-$	755.2039	755.2040	0.13	609, 547, 489, 393, 301, 300, 229, 179, 103	https://www.ncbi.nlm.nih.gov/pubmed/25383680
Quercetin-glucoside	6.915	$C_{12}H_{19}O_{12}^-$	463.0877	463.0875	−0.43	343, 301, 300, 207, 151	https://www.ncbi.nlm.nih.gov/pubmed/27842248
Kaempferol-glucoside	7.231	$C_{21}H_{19}O_{11}^-$	447.0933	447.0928	−1.11	363, 327, 284, 285, 227, 151	https://www.hindawi.com/journals/bmri/2013/345465/
Apigenin-glucoside-arabinoside	7.348	$C_{26}H_{27}O_{14}^-$	563.1406	563.1402	−0.71	518, 474, 430, 385, 333, 284, 181, 130	https://www.ncbi.nlm.nih.gov/pubmed/18686968

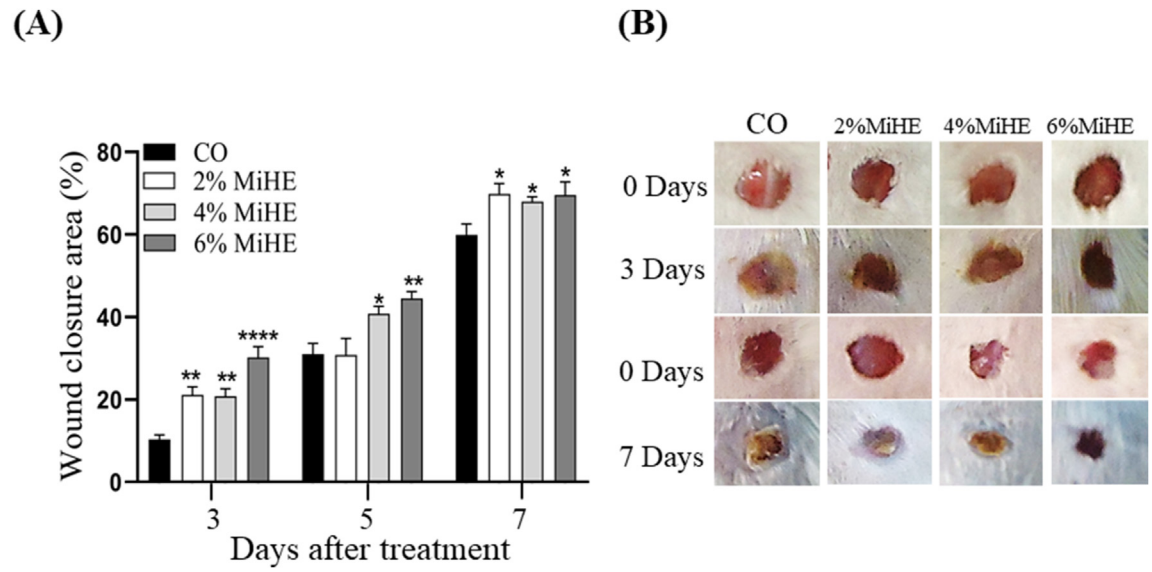

Fig. 1. Wound closure area. (A) Graphical representation of the percentage of wound closure treated with *M. ilicifolia* hydroethanolic extracts at concentrations of 2% (2% MiHE), 4% (4% MiHE) and 6% (6% MiHE) and animals injured and treated with vehicle (group CO), after 3 and 7 days of treatment. (B) Macroscopic images of wound closure immediately after wound induction (day 0) and after 3 and 7 days of treatment. The results are shown as mean and standard error, statistically evaluated with One-Way ANOVA and Bonferroni post-tests ($n = 8$). * indicates a statistically difference in relation to CO group considering $p \leq 0.05$, **$p \leq 0.01$ and ****$p \leq 0.0001$.

of polyphenols represented by tannins (Type B proanthocyadinin (dimer); Type B procyanidin (dimer); Type B proanthocyanidin (trimer) and Type B proanthocyanidin (trimer)) and flavonoids ((Epi)gallocatechin; (Epi)catechin; Epiafzelechin; Quercetin-rutinoside-glucoside; Quercetin rhamnosylrutinoside; Quercetin-glucoside and Kaempferol-glucoside).

3.2. MiHE improves skin wound closure

Wounds treated with MiEH showed accelerated closure after 3 and 7 days of treatment (Fig. 1A and Fig. 1B). After 3 days of treatment, the percentages of wound area closure were greater in wounds treated with 2% MiHE (21.1 ± 1.1) ($p \leq 0.05$), 4% MiHE 20.8% ± 1.8 ($p \leq 0.05$) and 6% MiHE 30.2% ± 2.6 ($p \leq 0.01$) in relation to CO group (10.3% ± 1.1) (Fig. 1A and B). After 7 days of treatment, all concentrations of MiHE improved the wound closure ($p \leq 0.05$), with closure of 69.8% ± 2.5 (2% MiHE), 67.9% ± 1.2 (4% MiHE) and 69.5% ± 3.2 (6% MiHE) in comparison to CO group (60% ± 2.6) (Fig. 1A and B). Only wounds treated with 4% MiHE ($p \leq 0.05$) and 6% MiHE ($p \leq 0.01$) were different from the wounds of CO group (31.1% ± 2.6) after 5 days of treatment (40.8% ± 1.7 and 44.5% ± 2.6 of wound closure, respectively) (Fig. 1A and B).

3.3. MiHE has effect on the activity of neutrophils and macrophages

The treatments with 4% MiHE (53.4 ± 3.8) $p \leq 0.05$ and 6% MiHE (60.2 ± 5.6) ($p \leq 0.01$) showed reductions in MPO activity, when compared with CO group (53.4 ± 3.80) after 3 days of treatment (Fig. 2A). Otherwise, MPO activity was elevated in all groups treated with MiHE after 7 days of treatment, with 35.2 ± 7.3 ($p \leq 0.0001$) 2% MiHE, 17 ± 7 ($p \leq 0.0001$) 4% MiHE and 17.7 ± 2.4 ($p \leq 0.001$) 6% MiHE, in relation to CO group (3.1 ± 0.3) (Fig. 2A). After 3 days of treatment, NAG activity was reduced in 2% MiHE (5.3 ± 0.6) $p \leq 0.5$ and 4% MiHE (2.1 ± 0.1) $p \leq 0.01$ groups, when compared with CO group (8 ± 0.8), whereas, after 7 days of treatment, NAG activity was increased in the 4% MiHE group (8.7 ± 1) $p \leq 0.5$ in relation to CO group (5.5 ± 0.7). The treatment with 2% MiHE and 6% MiHE showed no differences in the NAG activity in relation to the CO group after 7 days of treatment (Fig. 2B).

3.4. MiHE treatment increases the number of mast cells and MMP-9 activity in wounds

The quantification of mast cells in wounds treated with MiHE was compared with the CO group (animals injured and treated with vehicle). After 3 days of treatment, an increase (1.2 ± 0.2) ($p \leq 0.05$) in the number of mast cells was observed in wounds treated with 4% MiHE in relation to CO group (0.6 ± 0.1). In the same period, the increase was of 1.3 ± 0.2 ($p \leq 0.01$) in the wounds treated with 6% MiHE (Fig. 3A and Fig. 3C). After 7 days of treatment, only the group 6% MiHE (0.9 ± 0.4) $p \leq 0.01$ showed an increase of mast cells in relation CO group (0.3 ± 0.1) (Fig. 3A and C).

After 3 days of treatment, there was no statistical difference of pro-MMP9 and active MMP-9 between MiHE (all concentrations) and CO group (Fig. 4A). Otherwise, after 7 days of treatment, pro-MMP-9 activity in wounds treated with 4% MiHE (1.297 ± 38) $p \leq 0.01$ and 6% MiHE (1.2500 ± 131) $p \leq 0.01$ was greater than the activity for the CO group (460 ± 182). These same groups also showed increased MMP-9 activity with values of (917 ± 69) $p \leq 0.05$ and (973 ± 143) $p \leq 0.01$, respectively) after 7 days of treatment, compared with CO group (558 ± 74) (Fig. 4B). Pro-MMP2 and active MMP2 were observed only in wounds treated for 3 days, and were not statistically different between MiHE and CO group (Fig. 4C).

3.5. MiHE presents pro-angiogenic and pro-fibrogenic activities in skin wounds

Hemoglobin content in skin wounds increased in 4% MiHE (13.1 ± 2) ($p \leq 0.0001$) compared to the CO group (6.4 ± 1.20) at the beginning of wound repair (after 3 days of treatment) (Fig. 5A). At the end of the experimental treatments, the hemoglobin value in 4% MiHE was reduced (3.7 ± 0.3) $p \leq 0.01$ in relation to the CO group (7.6 ± 0.4) (Fig. 5A).

After 3 days of treatment, only 4% MiHE exhibited increased total collagen deposition (292 ± 63) $p \leq 0.05$ (Fig. 5B and B) and soluble collagen (3.0 ± 0.5) $p \leq 0.05$ in relation to the wounds treated with CO group (148 ± 39 of total collagen and 1.6 ± 0.3 of soluble collagen) (Fig. 5C). After 7 days of treatment, total collagen

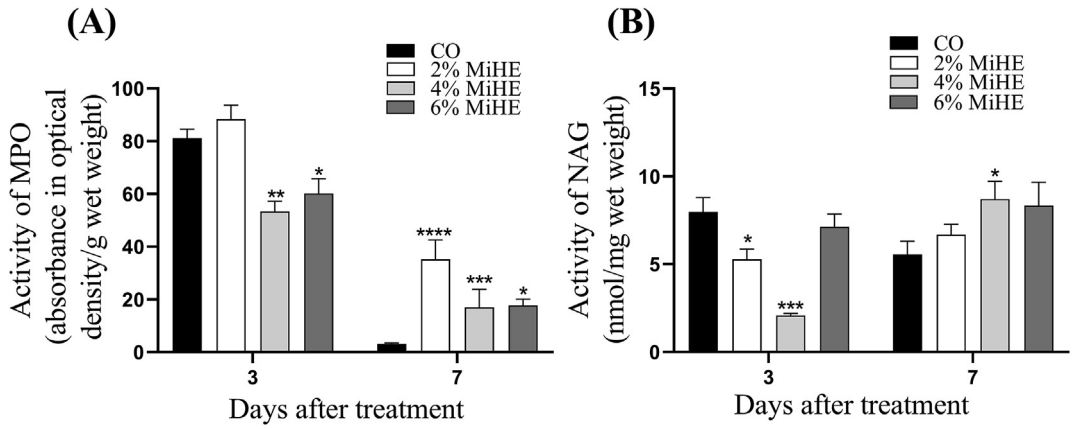

Fig. 2. Myeloperoxidase activity (neutrophil marker) and *N*-acetyl-β-D-glucosaminidase (macrophage marker). Graphical representation of MPO **(A)** and NAG **(B)** activities in wounds after 3 and 7 days of treatment with *M. ilicifolia* hydroethanolic extract at concentrations of 2% (2% MiHE), 4% (4% MiHE), and 6% (6% MiHE) and treated with vehicle (CO group). The results are shown as mean and standard error, statistically evaluated with One-Way ANOVA and Bonferroni post-tests (n = 8). * indicates statistically significant difference in relation to the control group considering $p \leq 0.05$, **$p \leq 0.01$, ***$p \leq 0.001$ and ****$p \leq 0.0001$.

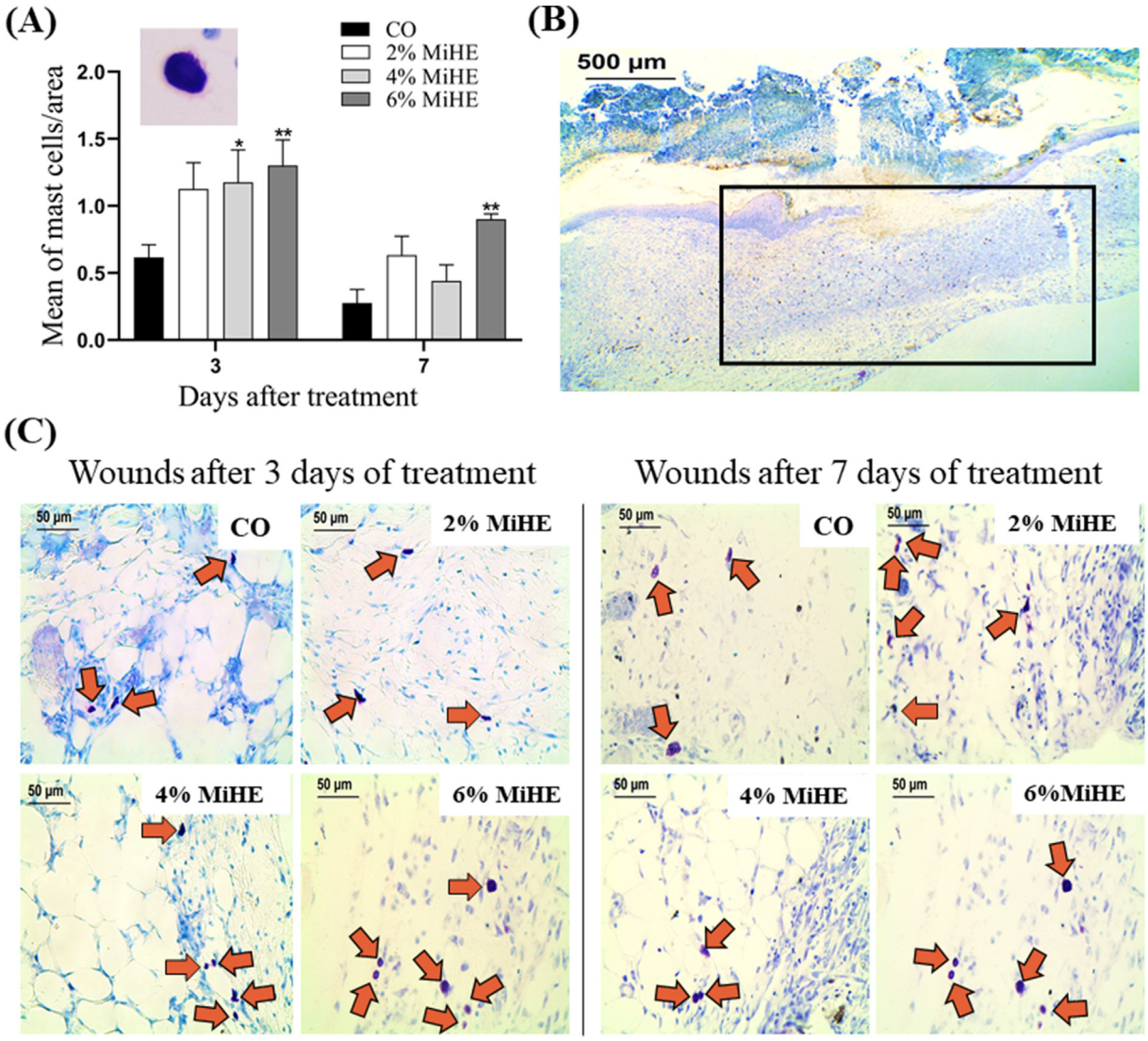

Fig. 3. Quantification of mast cells in wound areas stained with Toluidine Blue. (A) Quantification of mast cells in photomicrographs of cutaneous wounds after 3 and 7 days of treatment with *M. ilicifolia* hydroethanolic extract at concentrations of 2% (2% MiHE), 4% (4% MiHE) and 6% (6% MiHE) and vehicle-treated wounds (CO group). The results are shown as mean and standard error, statistically evaluated with One-Way ANOVA and Bonferroni post-tests (n = 8). * indicates statistical difference in relation to the CO group considering $p \leq 0.05$ and **$p \leq 0.01$. **(C)** Photomicrograph of skin wounds stained with Toluidine Blue after the treatment with mast cells indicated by the arrows. Photomicrograph **(A)** represents an enlarged mast cell about the graphic and **(B)** the injured tissue after 7 days of treatment. The delimited area (B) showing the region where the photomicrographs were personalized Photomicrographs are presented with the following magnitudes: (B) 40x and (C) 400x.

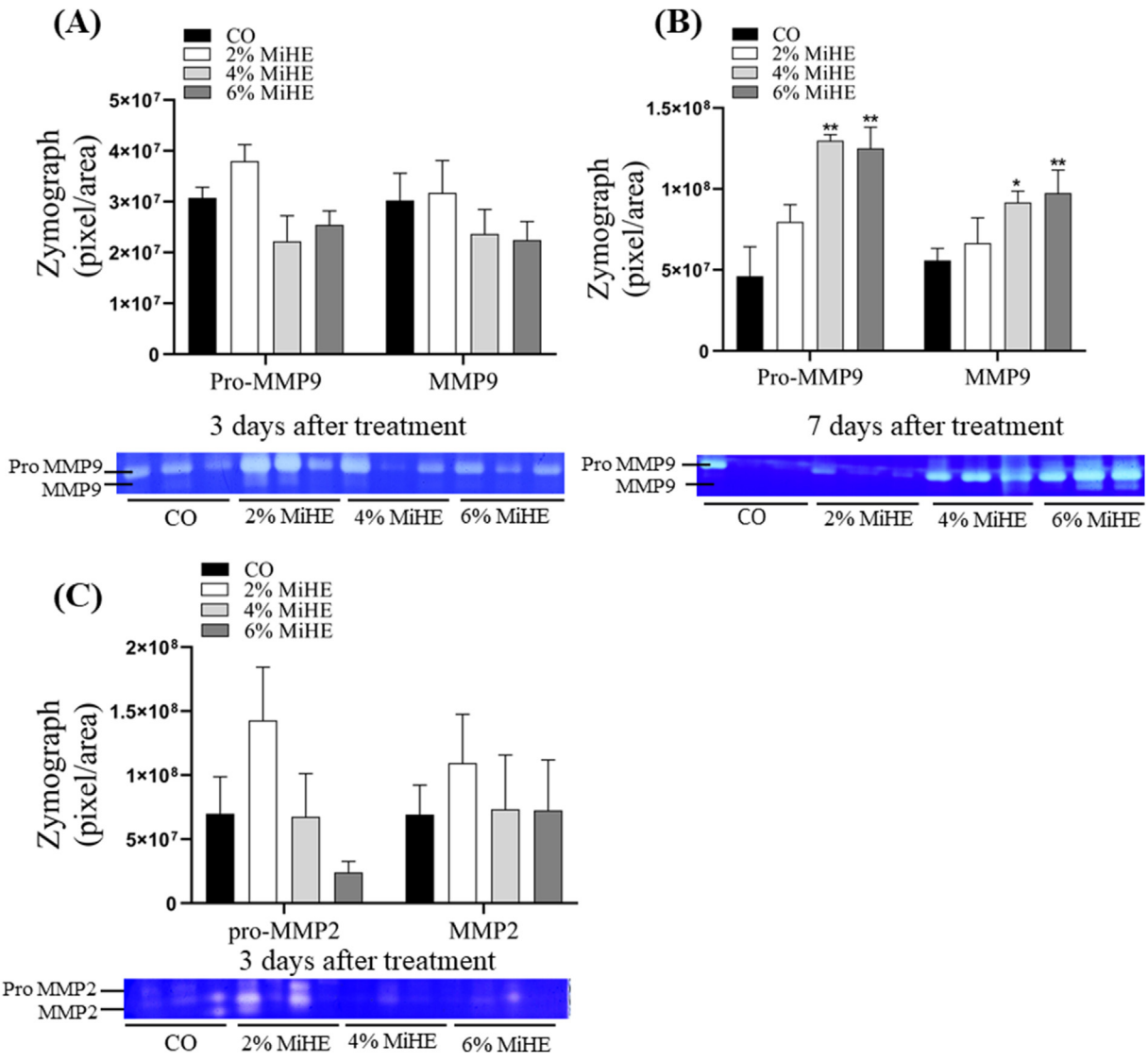

Fig. 4. Pro-MMPs and active MMPs quantification. Zymography gel and graphical representation of band densitometry of pro-MMP9 and active forms of MMP-9 after 3 **(A)** and 7 days **(B)** of treatment in CO group (animals injured and treated with vehicle) and *M. ilicifolia* hydroethanolic extract at concentrations of 2% (2% MiHE), 4% (4% MiHE) and 6% (6% MiHE). **(C)** Represents optical density from the bands obtained by the zymography gel for pro-MMP2 and active MMP2 after 3 days of treatment. The results are shown as mean and standard error, statistically evaluated with One-Way ANOVA and Bonferroni post-tests ($n = 3$). * indicates statistically significant difference in relation to the control group considering $p \leq 0.05$ and **$p \leq 0.01$.

increased (1346 ± 90) $p \leq 0.01$, (1288 ± 132) $p \leq 0.01$ and (1679 ± 91) $p \leq 0.001$, respectively, in wounds treated with 2% MiHE, 4% MiHE and 6% MiHE, compared with CO group (651 ± 194) (Figs. 5B and 6B). Considering soluble collagen, only the wounds treated with 4% MiHE showed increases in its content (2.4 ± 0.3) $p \leq 0.05$, in relation to the CO group (1.3 ± 0.1) (Fig. 5C). Wounds of the 4% MiHE (0.8 ± 0.02) $p \leq 0.1$ and 6% MiHE ($0.8 \leq 0.02$ $p \leq 0.01$) showed a predominance of type III collagen, compared with CO group (0.7 ± 0.01). There was no difference between the type I and III collagen ratio after 3 days of treatment (Figs. 5D and 6C).

4. Discussion

Wound healing involves a complex process that aims to restore the structural and/or functional integrity of damaged tissue. It is achieved through four precise and highly programmed phases: hemostasis, inflammation, proliferation and remodelling.[39] *M. ilicifolia* presents a diversity of polyphenols. Regarding the anti-inflammatory action of these compounds and the fact that we are not aware of studies that evaluate the effect of *M. ilicifolia* on skin wounds, in this study, we chose to focus on the initial stages: inflammation (3 days) and proliferation (7 days).

Among the compounds known for their healing activity, epigallocatechin and proanthocyanin were found in MiHE. Epigallocatechin has demonstrated activity on the proliferation of keratinocytes.[40] Moreover, this curative property can be developed as an action of tannins (such as proanthocyanin). This compound has astringent, anti-inflammatory and healing characteristics in the treatment of wounds and burns, forming a protective layer in the lesion and favouring the natural recovery of tissue.[15] Other polyphenols found in MiHE known for their healing activity are quercetin[41] and kaempferol,[42] which have been evaluated and presented positive results in terms of healing in different experimental models such as healthy, diabetic and pressure ulcer animals. In this study, we demonstrated that the healing activity of MiHE was accompanied by anti-inflammatory activity, pro-angiogenic activity and effects on the extracellular matrix with increased collagen and MMP expression.

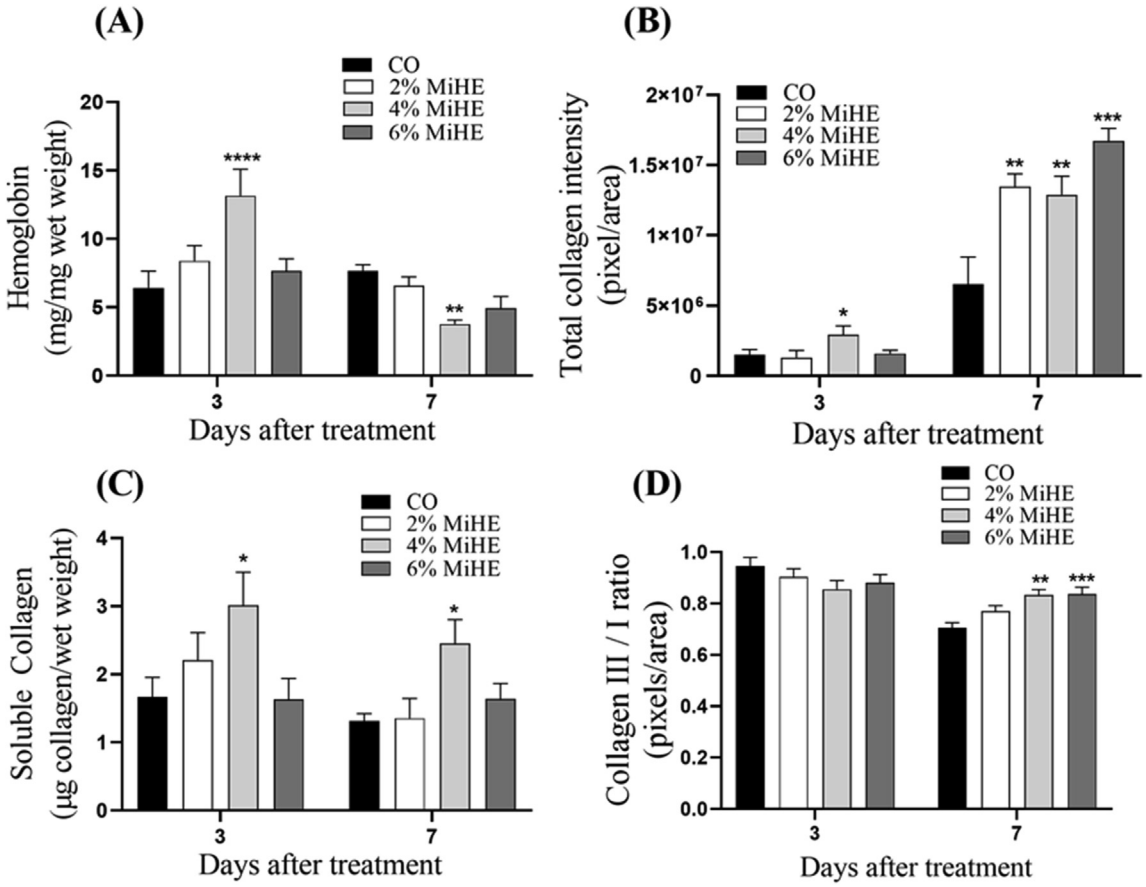

Fig. 5. Quantification of hemoglobin and collagen in wounds. Graphical representation of hemoglobin **(A),** total collagen deposition **(B)**, soluble collagen **(C)** and proportions of types I and III collagen **(D)**. All evaluations were carried out in wounds after 3 and 7 days of treatment with *M. ilicifolia* hydroethanolic extract at concentrations of 2% (2% MiHE), 4% (4% MiHE) and 6% (6% MiHE) and CO group (animals injured and treated with vehicle). The results are shown as mean and standard error, statistically evaluated with One-Way ANOVA and Bonferroni post-tests (n = 8). * indicates statistically significant difference in relation to the control group considering $p \leq 0.05$, **$p \leq 0.01$ and ***$p \leq 0.001$ and ****$p \leq 0.0001$.

Neutrophils are one of the main cells of the inflammatory stage of wound healing and play an important role in decontamination by eliminating foreign debris and promoting defence against infections.[43] Despite this, when they persist in wounds for a long time, neutrophil-derived mediators can cause damage to host tissues and potentially delay the repair process.[43] The indirect activity of neutrophils was obtained from the quantification of the enzyme MPO. Enzymatic activity was reduced in wounds treated with MiHE after 3 days of treatment.

Characterisation of MiHE demonstrated a wide variety of flavonoids, known as anti-inflammatory compounds.[10,44] Among the polyphenol groups described for MiHE, flavonoids were the most representative, presenting (epi)gallocatechin, (epi)catechin, epiafzelechin, quercetin-rutinoside-glucoside, quercetin rhamnosylrutinoside, quercetin-glucoside, kaempferol-glucoside and apigenin-glucoside-arabinoside. Flavonoids have been evaluated for their inhibitory activity on MPO. This inhibitory role is associated with the position of the hydroxyl, the ability to eliminate free radicals and the hydrophobicity of the molecule.[44] In addition to their action on MPO, flavonoids may have anti-inflammatory activity through alternative mechanisms, as for epiafzelechin which exhibits anti-inflammatory activity on carrageenin-induced mouse paw oedema by inhibiting the cyclooxygenase (COX)-1 activity of prostaglandin H_2 synthase.[45] MiHE features glycoside flavonoids, among them kaempferol-glucoside. This compound has anti-inflammatory and analgesic activity in part due to its ability to reduce the migration of leukocytes.[46] In our previous studies, we demonstrated that wounds treated with an extract rich in glycoside and rutinoside flavonoids such as quercetin-glucoside, kaempferol-rutinoside and kaempferol-glucoside, compounds also present in MiHE, were able to reduce the activity of MPO.[10]

We demonstrated that wounds treated with MiHE have reduced neutrophil activity after 3 days of treatment and increased this activity after 7 days when compared with the CO group (control group). However, neutrophil activity was reduced in these groups (2% MiHE **, 4% MiHE ** and 6% MiHE ***) after 7 days when compared to the same group in a shorter time, after 3 days of treatment (statistics not shown on the graph). In addition, although MPO is widely used as a marker of neutrophil activity, it can also be produced by macrophages,[47] which may have contributed to the increase in MPO in relation to the CO group after 7 days of treatment. These results suggest that wounds treated for 7 days with 4% MiHE showed a profile of resolution of the inflammatory process and a direction for the proliferative stage. This is because the reduction of neutrophils over time (between 3 and 7 days of treatment) occurred simultaneously with an increase in macrophage activity. Macrophages are essential for the progression of the repair process, as they eliminate neutrophils by phagocytosis while producing essential mediators for the proliferative stage.[39]

MMPs play a key role in the proliferation stage. Interactions between mast cells and fibroblasts induce MMP-9 release from fibroblasts.[48] Mast cell chymase is involved in the activation of pro-

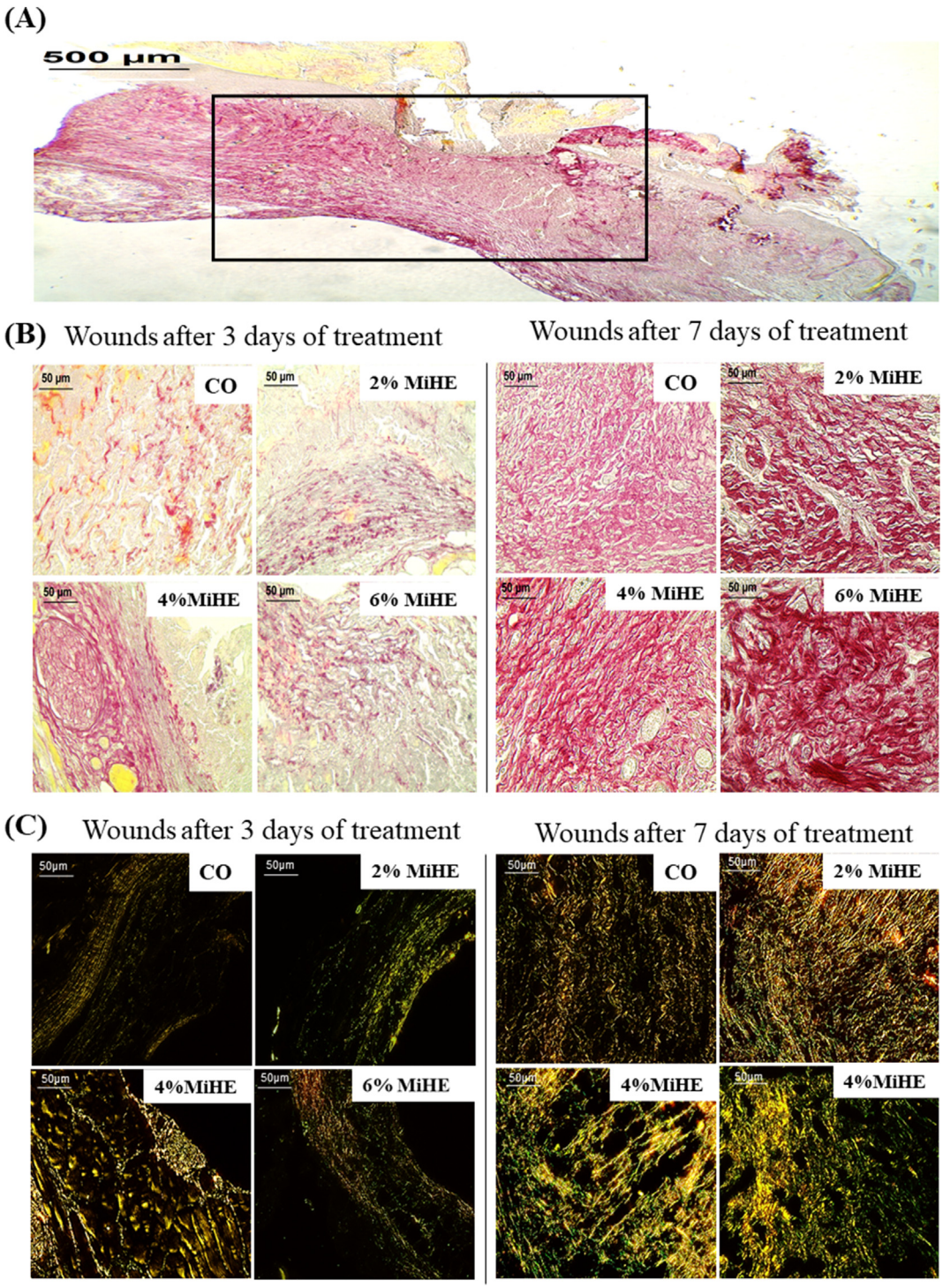

Fig. 6. Total collagen deposited on the extracellular matrix of the wound area. Photomicrograph of skin wounds stained with Sirius Red showing total collagen **(B) and collagen types I and III (C)** in wound of CO group (vehicle-treated wounds) and *M. ilicifolia* hydroethanolic extract at concentrations of 2% (2% MiHE), 4% (4% MiHE) and 6% (6% MiHE) after 3 and 7 days of treatment. In the photomicrographs shown in (C), type I collagen is observed in orange-red, while type III collagen is observed in green. The delimitation (rectangle) in the upper image **(A)** represents the area where the images were obtained. Photomicrographs are presented with the following magnitudes: (A) 40x, (B) and (C) 400x.

MMP9[49] and tryptase-producing mast cells may be associated with MMP-9 expression.[48] Thus, in our study, we suggest that the increase in mast cells in wounds treated with 4% MiHE and 6% MiHE after 3 days of treatment may have resulted in an increase in mediators that led to an increase in MMP-9 expression by fibroblasts in the following days (observed after 7 days of treatment).

MMP-9 is a fundamental protease for keratinocyte activity, including their migration and re-epithelialisation.[50] MMP-9 is expressed at the contact edges of keratinocytes that migrate during wound closure. Thus, an increase in MMP-9 activity with topical treatments containing MiHE may reduce the time required for wound closure, due to its activity on cells that promote re-epithelialisation. Moreover, MMP9-knockout animals exhibit a delay in wound closure.[51] Regarding MMP-2, it has been shown

that its expression in the wound filling region is characteristic during the inflammatory stage.[52] For this reason, we could only identify MMP-2 activity in samples obtained after three days of treatment, which represents the inflammatory stage of healing.

Angiogenesis and collagen production are also characteristic processes of the proliferative phase. Angiogenesis starts approximately from day 4 after the injury[53] and delivers oxygen, nutrients and essential growth factors to the injured skin tissue, facilitating the healing process. In this study, we used hemoglobin quantification as an evaluation method for angiogenesis. 4% MiHE led to an increase in the hemoglobin content after day 3 of treatment, followed by a reduction after 7 days of treatment, which can lead to tissue maturation. This is because, considering the physiological processes involved in healing, after an increase in blood vessels, blood vessels regress until they reach the density of blood vessels characteristic of normal skin, without lesions.[39] Some of the compounds present in MiHE with proven angiogenic activity, such as the catechins, can up-regulate the enzyme nitric oxide synthase.[54] As previously shown, treatment with 4% MiHE for 3 days after lesion induction also induced the accumulation of mast cells near the wound site. During the healing process, mast cell infiltration can contribute to angiogenesis through the secretion of cytokines, such as vascular endothelial growth factor (VEGF) and fibroblast growth factor (FGF), or by the release of pre-stocked proteases in their granules (e.g. tryptase). Both processes are capable of positively modulating the neovascularisation of wounds.[55,56,57]

Total collagen and soluble collagen increases were observed in the 4% MiHE group, after days 3 and 7 of treatment. This provides integrity and resistance to the tissue. Furthermore, it contributes to better cell migration in the proliferative and remodelling phases,[58] resulting in a reduced the time for wound closure treated with 4% MiHE. Compounds present in MiHE show pro-fibrogenic activity. Flavonol glycosides have previously been shown to stimulate fibroblast proliferation and collagen synthesis,[59,60] while glycosylated kaempferol and kaempferol exert an effect on collagen synthesis, demonstrated by an increase in hydroxyproline and total collagen, respectively.[10,42] The main collagen constituents of the dermis are collagen types I and III. The study of these fibres is essential because it indicates the degree of maturation of the formed tissue. After 7 days of treatment, wounds treated with MiHE showed a predominance of type III collagen. Maximum type III collagen production occurs between 5 and 7 days after injury.[61] Thus, the increase in this collagen in wounds treated with MiHE indicates adequate progression in the healing process. Type III collagen plays a fundamental role in granulation tissue, contributing to the migration and proliferation of cells such as keratinocytes and fibroblasts,[62] resulting in adequate fibrogenesis and a shorter wound closure time.

5. Conclusion

4% MiHE was efficient at accelerating wound closure. 4% MiHE demonstrated anti-inflammatory, pro-angiogenic and pro-fibrogenic activity. Moreover, the increase in MMP-9 contributes to the advancement of the proliferative stage, since MMP-9 is fundamental for the keratinisation process and for epidermal closure. Thus, this study has shown that 4% MiHE presents beneficial properties and may be an interesting option for accelerating skin wound healing.

Funding sources

This study was financed by the Coordenação de Aperfeiçoamento de Pessoal de Nível Superior - Brasil (CAPES) - Finance Code 001, Fundação de Amparo à Pesquisa do Estado de Minas Gerais FAPEMIG) and Conselho Nacional de Desenvolvimento Científico e Tecnológico (CNPq) and the National Institute of Science and Technology in Theranostics and Nanobiotechnology—INCT-TeraNano (CNPq/CAPES/FAPEMIG, CNPq-465669/2014–0 and FAPEMIG-CBB-APQ-03613-17).

Declaration of competing interest

The authors declare that they have no competing interests.

Acknowledgements

Thank the Rede de Biotérios de Roedores (REBIR) of Federal University de Uberlândia (UFU), who contributed to the supply, willingness to develop the experimental model, fulfilling the requirements relating to animal houses and always preserving animal welfare.

Appendix A. Supplementary data

Supplementary data to this article can be found online at https://doi.org/10.1016/j.jtcme.2021.03.003.

References

1. Cañedo-Dorantes L, Cañedo-Ayala M. Skin acute wound healing: a comprehensive review. *Int J Inflamm*. 2019:1–15.
2. Aplleton I. Wound healing: future directions. 2003;6(11):1067–1072.
3. Nussbaum SR, Carter MJ, Fife CE, et al. An economic evaluation of the impact, cost, and medicare policy implications of chronic nonhealing wounds. *Value Health*. 2018;21(1):27–32.
4. Heyer K, Herberger K, Protz K, et al. Epidemiology of chronic wounds in Germany: analysis of statutory health insurance data. *Wound Repair Regen*. 2016;24(2):434–442.
5. Guest JF, Ayoub N, McIlwraith T, et al. Health economic burden that wounds impose on the National Health Service in the UK. *BMJ Open*. 2015;5(12):1–9.
6. Mantle D, Gok M, Lennard T. Adverse and beneficial effects of plant extracts on skin and skin disorders. *Adverse Drug React Toxicol Rev*. 2021;20(2):89–103.
7. Newman DJ, Cragg GM. Natural products as sources of new drugs from 1981 to 2014. *J Nat Prod*. 2016;79(3):629–661.
8. Gharaboghaz MNZ, Farahpour MR, Saghaie S. Topical co-administration of *Teucrium polium* hydroethanolic extract and *Aloe vera* gel triggered wound healing by accelerating cell proliferation in diabetic mouse model. *Biomed Pharmacother*. 2020;127:110189.
9. Farahpour MR, Sheikh S, Kafshdooz E, Sonboli A. Accelerative effect of topical *Zataria multiflora* essential oil against infected wound model by modulating inflammation, angiogenesis, and collagen biosynthesis. *Pharm Biol*. 2021;59(1):1–10.
10. De Moura FBR, Justino AB, Ferreira BA, et al. Pro-fibrogenic and anti-inflammatory potential of a polyphenol-enriched fraction from *Annona crassiflora* in skin repair. *Planta Med*. 2019;85(7):570–577.
11. Almeida C, Barbieri RL, Ribeiro MV, et al. Espinheira-santa (*Maytenus ilicifolia* Mart. ex Reiss.): saber de erveiros e feirantes em Pelotas (RS). *Rev Bras Plantas Med*. 2015;17(4):722–729.
12. Jorge RM, Leite JPV, Oliveira AB, et al. Evaluation of antinociceptive, anti-inflammatory and antiulcerogenic activities of *Maytenus ilicifolia*. *J Ethnopharmacol*. 2004;94(1):93–100.
13. Wang J, Fang X, Ge L, et al. Antitumor, antioxidant and anti-inflammatory activities of kaempferol and its corresponding glycosides and the enzymatic preparation of kaempferol. *PloS One*. 2018;13(5):1–12.
14. Seifried HE, Anderson DE, Fisher EI, et al. A review of the interaction among dietary antioxidants and reactive oxygen species. *J Nutr Biochem*. 2007;18(9):567–579.
15. Zhao X, Ai Y, Hu Y, et al. Masking the perceived astringency of proanthocyanidins in beverages using oxidized starch hydrogel microencapsulation. *Foods*. 2020;9(6):756.
16. Júnior RFA, Oliveira ALCSL, Pessoa JB, et al. *Maytenus ilicifolia* dry extract protects normal cells, induces apoptosis and regulates Bcl-2 in human cancer cells. *Exp Biol Med*. 2013;238(11):1251–1258.
17. Wonfor R, Natoli M, Parveen I, et al. Anti-inflammatory properties of an extract of *M. ilicifolia* in the human intestinal epithelial Caco-2 cell line. *J Ethnopharmacol*. 2017;209:283–287.
18. Tabach R, Duarte-Almeida JM, Carlini EA. Pharmacological and toxicological study of *Maytenus ilicifolia* leaf extract Part II—clinical study (phase I). *Phyther Res*. 2017;31(6):921–926.
19. Cunha-Laura AL, Auharek SA, Oliveira RJ, et al. Effects of *Maytenus ilicifolia* on reproduction and embryo-fetal development in Wistar rats. *Genet Mol Res*.

2014;13(2):3711–3720.
20. Ecker A, Loss CG, Adefegha SA, et al. Safety evaluation of supratherapeutic dose of *Maytenus ilicifolia* Mart. ex Reissek extracts on fertility and neurobehavioral status of male and pregnant rats. *Regul Toxicol Pharmacol*. 2017;90:160–169.
21. Heijmen FH, Du Pont JS, Middelkoop E, et al. Cross-linking of dermal sheep collagen with tannic acid. *Biomaterials*. 1997;18(10):749–754.
22. Habibi Zadeh S, Farahpour M, Kar HH. The effect of topical administration of an ointment prepared from *Trifolium repens* hydroethanolic extract on the acceleration of excisional cutaneous. *Wound Heal*. 2020;32(9):253–261.
23. Daemi A, Farahpour MR, Oryan A, et al. Topical administration of hydroethanolic extract of *Lawsonia inermis* (Henna) accelerates excisional wound healing process by reducing tissue inflammation and amplifying glucose uptake. *Kaohsiung J Med Sci*. 2019;35(1):24–32.
24. Barbosa JS, Moura FBR, Ferreira BA, et al. Recombinant protein rP21 from *Trypanosoma cruzi* has effect on inflammation , angiogenesis and fibrogenesis in skin wound model C57BL/6 mouse. 2021;22(1):28–37.
25. Salehi M, Ehterami A, Farzamfar S, et al. Accelerating healing of excisional wound with alginate hydrogel containing naringenin in rat model. *Drug Deliv Transl Res*. 2021;11(1):142–153.
26. Pinto N de CC, Cassini-Vieira P, Souza-Fagundes EM, et al. *Pereskia aculeata* Miller leaves accelerate excisional wound healing in mice. *J Ethnopharmacol*. 2016;194:131–136.
27. Barcelos L, Talvani A, Teixeira A, et al. Impaired inflammatory angiogenesis , but not leukocyte influx , in mice lacking TNFR1. *J Leukoc Biol*. 2005;78(2):352–358.
28. Cassini-Vieira P, Moreira CF, Da Silva MF, et al. Estimation of wound tissue neutrophil and macrophage accumulation by measuring myeloperoxidase (MPO) and N-Acetyl-β-D-glucosaminidase (NAG) activities. *Bio-Protocol*. 2015;5(22), e1662.
29. Ferreira BA, Norton Filho AF, Deconte SR, et al. Sesquiterpene polygodial from *Drimys brasiliensis* (winteraceae) down-regulates implant-induced inflammation and fibrogenesis in mice. *J Nat Prod*. 2020;83(12):3698–3705.
30. Silva SA, Gobbo MG, Pinto-Fochi ME, et al. Prostate hyperplasia caused by long-term obesity is characterized by high deposition of extracellular matrix and increased content of MMP-9 and VEGF. *Int J Exp Pathol*. 2015;96(1):21–30.
31. Esquisatto MAM, De Aro AA, Fèo HB, et al. Changes in the connective tissue sheath of Wistar rat nerve with aging. *Ann Anat*. 2014;196(6):441–448.
32. Bradford M. A rapid and sensitive method for the quantitation of microgram quantities of protein utilizing the principle of protein-dye binding. *Anal Biochem*. 1976;72:248–254.
33. Hu D, Hiley C, Smither R, et al. Correlation of 133Xe clearance, blood flow and histology in the rat sponge model for angiogenesis. Further studies with angiogenic modifiers. *Lab Invest*. 1995;72(5):601–610.
34. Plunkett M, Hailey J. An *in vivo* quantitative angiogenesis model using tumor cells entrapped in alginate. *Lab Invest*. 1990;62(4):510–517.
35. Seifert AW, Maden M. New insights into vertebrate skin regeneration. *Int Rev Cell Mol Biol*. 2014;310:129–169.
36. Junqueira LC, Bignolas G, Brentani R. Picrosirius staining plus polarization microscopy, a specific method for collagen detection in tissue sections. *Histochem J*. 1979;11:447–455.
37. Phillips RJ, Burdick MD, Hong K, et al. Circulating fibrocytes traffic to the lungs in response to CXCL12 and mediate fibrosis. *J Clin Invest*. 2004;114(3):438–446.
38. Campos PP, Bakhle YS, Andrade SP. Mechanisms of wound healing responses in lupus-prone New Zealand White mouse strain. *Wound Repair Regen*. 2008;16(3):416–424.
39. Reinke JM, Sorg H. Wound repair and regeneration. *Eur Surg Res*. 2012;49(1):35–43.
40. Klass BR, Branford OA, Grobbelaar AO, et al. The effect of epigallocatechin-3-gallate, a constituent of green tea, on transforming growth factor-β1-stimulated wound contraction. *Wound Repair Regen*. 2010;18(1):80–88.
41. Yin G, Wang Z, Wang Z, et al. Topical application of quercetin improves wound healing in pressure ulcer lesions. *Exp Dermatol*. 2018;27(7):779–786.
42. Özay Y, Güzel S, Yumrutaş Ö, et al. Wound healing effect of kaempferol in diabetic and nondiabetic rats. *J Surg Res*. 2019;233:284–296.
43. Wilgus TA, Roy S, McDaniel JC. Neutrophils and wound repair: positive actions and negative reactions. *Adv Wound Care*. 2013;2(7):379–388.
44. Shiba Y, Kinoshita T, Chuman H, et al. Flavonoids as substrates and inhibitors of myeloperoxidase: Molecular actions of aglycone and metabolites. *Chem Res Toxicol*. 2008;21(8):1600–1609.
45. Miri KR, Hwang BY, Lim' H-S, et al. (—)-Epiafzelechin: cyclooxygenase-1 inhibitor and anti-inflammatory agent from aerial parts of Celastrus orbiculatus. *Planta Med*. 1999;65:460–462.
46. De Melo GO, Malvar DC, Vanderlinde FA, et al. Antinociceptive and anti-inflammatory kaempferol glycosides from *Sedum dendroideum*. *J Ethnopharmacol*. 2009;124(2):228–232.
47. Loria V, Dato I, Graziani F, et al. Myeloperoxidase: a new biomarker of inflammation in ischemic heart disease and acute coronary syndromes. *Mediat Inflamm*. 2008:1–4.
48. Abel M, Vliagoftis H. Mast cell-fibroblast interactions induce matrix metalloproteinase-9 release from fibroblasts: role for IgE-mediated mast cell activation. *J Immunol*. 2008;180(5):3543–3550.
49. Tchougounova E, Lundequist A, Fajardo I, et al. A key role for mast cell chymase in the activation of pro-matrix metalloprotease-9 and pro-matrix metalloprotease-2. *J Biol Chem*. 2005;280(10):9291–9296.
50. Häkkinen L, Uitto V-J, Larjava H. Cell biology of gingival wound healing. *Periodontol*. 2000;24(1):127, 2000.
51. Hattori N, Mochizuki S, Kishi K, et al. MMP-13 plays a role in keratinocyte migration, angiogenesis, and contraction in mouse skin wound healing. *Am J Pathol*. 2009;175(2):533–546.
52. Caley MP, Martins VLC, O'Toole EA. Metalloproteinases and wound healing. *Adv Wound Care*. 2015;4(4):225–234.
53. Goldberg SE, Diegelmann RF. Basic science of wound healing. *Crit Limb Ischemia*. 2017;117:131–135.
54. Kapoor M, Howard R, Hall I, et al. Effects of epicatechin gallate on wound healing and scar formation in a full thickness incisional wound healing model in rats. *Am J Pathol*. 2004;165(1):299–307.
55. Komi DEA, Khomtchouk K, Santa Maria PL. A review of the contribution of mast cells in wound healing: involved molecular and cellular mechanisms. *Clin Rev Allergy Immunol*. 2019:1–15.
56. Blair RJ, Meng H, Marchese MJ, et al. Human mast cells stimulate vascular tube formation. Tryptase is a novel, potent angiogenic factor. *J Clin Invest*. 1997;99(11):2691–2700.
57. Farahpour MR, Mirzakhani N, Doostmohammadi J, et al. Hydroethanolic *Pistacia atlantica* hulls extract improved wound healing process; evidence for mast cells infiltration, angiogenesis and RNA stability. *Int J Surg*. 2015;17:88–98.
58. Barker TH. The role of ECM proteins and protein fragments in guiding cell behavior in regenerative medicine. *Biomaterials*. 2011;32(18):4211–4214.
59. Stipcevic T, Piljac J, Berghe DV. Effect of different flavonoids on collagen synthesis in human fibroblasts. *Plant Foods Hum Nutr*. 2006;61(1):29–34.
60. Koganov MM, Dueva OV, Tsorin BL. Activities of plant-derived phenols in a fibroblast cell culture model. *J Nat Prod*. 1999;62(3):481–483.
61. Li J, Zhang YP, Zarei M, et al. A topical aqueous oxygen emulsion stimulates granulation tissue formation in a porcine second-degree burn wound. *Burns*. 2015;41(5):1049–1057.
62. Kim JK, Xu Y, Xu X, et al. A novel binding site in collagen type III for integrins α1β1 and α2β1. *J Biol Chem*. 2005;280(37):32512–32520.